Acquisition of the head-centered peri-personal spatial representation found in VIP neuron

Sawa Fuke, Masaki Ogino, and Minoru Asada

***Abstract*—Both body and visuo-spatial representations are supposed to be gradually acquired during the developmental process as described in cognitive and brain sciences. A typical example is face representation in a neuron (found in the adjacent ventral intraparietal (in short, VIP) area) of which the function is not only to code for the location of visual stimuli in the head-centered reference frame but also to connect visual sensation with tactile sensation. This paper presents a model that enables a robot to acquire such representation. The proprioception of arm posture is utilized as reference data through the "hand regard behavior", that is, the robot moves its hand in front of its face, and self organizing map (SOM) and Hebbian learning methods are applied. The simulation results are shown and discussions on the limitation of the current model and future issues are given.**

***Index Terms*—Body representation, VIP neuron, Sensor fusion, Learning and adaptive system**

I. Introduction

Acquiring body representation is the most fundamental issue not only for robotics, in order to accomplish different kinds of tasks, but also for cognitive and brain sciences and related disciplines, since how humans acquire such representation is one of the great unresolved issues of human cognitive development. General consensus of body representation is roughly categorized into two types: "body schema," an unconscious neural map in which multi-modal sensory data are unified, and "body image," an explicit mental representation of the body and its functions [1][2]. The body representations in biological systems are apparently flexible and acquired by spatio-temporal integration of different information from different sensory modalities (ex., [3],[4]).

Among different modalities, vision is the most representative spatial perception that is expressed in various kinds of reference frames in different brain regions. A typical example is that the visual stimulus of a target is perceived in a retinotopic manner [5]. On the other hand, the adjacent ventral intraparietal (in short, VIP) area includes neurons which encode bimodal sensory information in a head-centered space coordinate system [6][7][8]. They are supposed to play an important role for the avoidance of obstacles and projectiles. Not only tactile stimuli on the face but surprisingly also visual stimuli, whose locations can be expressed in a head-centered reference frame regardless of ocular angles, can activate these neurons. Figure 1 shows examples of the visual and somatosensory receptive fields of the same neuron, which are not affected by gaze directions.

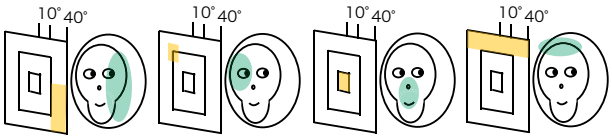

Fig. 1. Visual and somatosensory receptive fields of neurons in VIP. The same VIP neuron is activated when something is shown on the screen's shaded area in front of the monkey and when the face's shaded area is stimulated regardless of where the monkey is fixating (adapted from Figure 1 in [6])

We may hypothesize that in the brain the locations of visual stimuli on the retina are transformed to the locations in the abstract reference frames by integrating them with the proprioception (ex. neck and ocular angles) and associated with other sensor information (ex. tactile sense). Intriguingly, it is suggested that not only the body image (schema), but also this transformation system between reference frames in the visuo-space is also adaptively acquired through experiences (ex. [9]). However, the way humans acquire such representations in the brain in spite of the changes in body structures and sensitivities has remained an issue to be revealed.

A number of synthetic approaches aiming at understanding the acquisition process of body and visuo-spatial representation in humans have been attempted in cognitive developmental robotics [10], where the self-body or body parts are found or identified based on invariance in the sensor data [11], synchronization of motion and perception [12][13], Jacobian estimation [14], and reference frame transformation [15]. In these studies, the representation of invisible body parts such as a face or a back cannot be acquired because the robot cannot detect the visual information of the surface directly with their own cameras. Fuke et al. [16] proposed a model that acquired the body representation of a robot's invisible face by estimating its hand position from the change of the proprioception while touching its own face. However, these studies assumed that camera positions are fixed or that the coordinate system in visual space is given by the designer.

As a learning model of visuo-spatial representation, Pouget et al. [17] proposed an approach based on a neural network with statistically distributed input data so that multi-modal sensations can be integrated. However, they have not discussed what kind of information can be used to select the signals pertaining to the same location of the target. In fact, as shown in Figure 2, adult humans can recognize that a stationary object

Sawa Fuke, and Minoru Asada are with the Department of Adaptive Machine Systems, Graduate School of Engineering, Osaka University, Japan [sawa.fuke, asada]@ams.eng.osaka-u.ac.jp

Masaki Ogino is a researcher of Asada Synergistic Intelligence Project, ERATO, Japan ogino@jeap.org

Minoru Asada is a research director of Asada Synergistic Intelligence Project, ERATO.

is located in the same position though ocular angles and retina image are different when we detect it in the peripheral visual field.

Aiming at revealing the above issue, through the process of mutual feedback between hypothesis generation and its verification, here we propose a learning model in which a robot acquires not only the head-centered reference frame but also the cross-modal representation of the face based on the knowledge in neurophysiological and cognitive science, by focusing on a "hand regard" behavior that infants around 4-months often show. Eventually, we hope that the properties of acquired cross-modal representation are similar to the one of VIP neurons found in neuroscience. The proprioception of arm posture is utilized as reference data through the "hand regard" behavior, that is, the robot moves its hand in front of its face, while self organizing map (SOM) and Hebbian learning methods are applied. The SOM algorithm was proposed by Kohonen [18] who suggested that cortical maps may self-organize in a nearest-neighbor relationship. Based on this assumption, Aflalo et al. [19] actually modeled motor cortex topography using a Kohonen SOM and argued that their maps resembled the actual maps obtained from the lateral motor cortex of monkeys. Here, we used SOM for data compression. The simulation results are shown and discussions on the limitation of the current model and future issues are given.

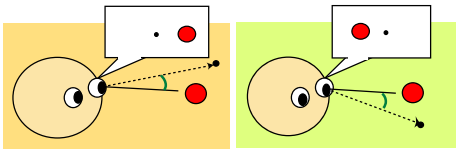

Fig. 2. In these two situations, we humans can recognize that the red objects locate at the same position though ocular angles and retina image are different when we detect it in the peripheral visual field. Actually, when we see something, there are many different sets of perceived information (ex. ocular angles and retina image).

II. Findings in Developmental Science Concerning the Visuo-Spatial Representation

Observation study suggests that the visual abilities of human infants develop dramatically from the age of 3 to 7 months old. The 3-month-old infants tend to plan saccades based on the retinocentric reference frame, ignoring the target shift due to eye movements. On the other hand, the 7-month-old infants do not ignore it [20]. This implies that human infants do not seem to have the visuo-spatial representation within certain reference frame systems from the beginning but acquire it through their experiences while their strength of muscles, and sensitivity and placement of sensory organs continue to change. While these visual abilities develop, a typical infant behavior called "hand regard" [21] is observed. "Hand regard" is the phenomenon in which 3 or 4-month-old infants often gaze at their own hands in front of their faces. Among many interpretations of this phenomenon, Rizzolatti et al. [22] suggest that it is probably to be ascribed to the necessity of calibrating "peri-personal space" (defined as the space within reach of the arm [23]) around a body by combining the motor and visual information. The VIP area in the parietal cortex is known as the region that contains this peri-personal visuo-spatial representation.

Considering these observations of infants, we propose a learning model that starts from the retinocentric representation to head-centered representation through "hand regard" behavior as shown Table 1. Then, we approach the issue of identifying what actual mechanism leads to the development of the visuo-spatial representation develop in the infant's brain. In our simulation, a robot learns the association between the tactile representation of the face and the learned visuo-spatial representation which enables the robot to show the reflexive behavior like the VIP neurons.

III. VIP Neuron Model

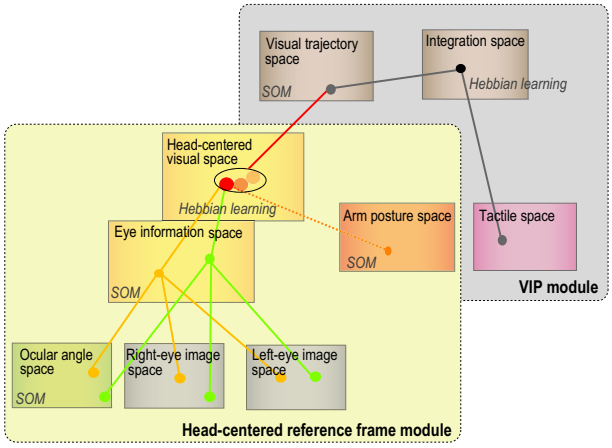

Fig. 3. An overview of the proposed model

An overview of the proposed model is shown in Figure 3, where two modules are involved. First, the robot acquires the head-centered reference frame module. It has many sets of ocular angles and the retinotopic images (camera images) that are represented in the eye information space in Figure 3. In order to construct a head-centered reference frame, the robot associates the ocular angles and camera images by regarding the proprioception of its own body (joint angles of the arm) as the reference information.

Next, in the VIP module, the robot integrates the tactile sensation with the patterns of visual stimuli computed in the head-centered reference frame in the former trained module when it touches its own face with its hand. Finally, the robot can acquire the cross-modal representation of its own face. The details of the robot simulator used and the details of each module are given in the following sections A, B, and C, respectively.

A. Robot simulator

In order to validate the model, computer simulations were conducted with a dynamic simulator based on the method of Featherstone [24]. The robot model used in this experiment and its specifications are shown in Figure 4. It has arms with five degrees of freedom. Furthermore, it has a binocular vision

TABLE I
THE FINDINGS THAT SUPPORT THE CONDITIONS OF SIMULATION

Month	Observed behavior (infant)	Situation of the robot experiment
3	Saccadic movement in the retinocentric reference frame	Perceiving ocular angles and camera image data
3,4	"Hand regard" behavior	Moving its own hand and watching it
7	Saccadic movement in the body-centered reference frame	Integrating ocular angles and camera image data

system and each eye has two degrees of freedom (pan and tilt). The left hand is colored red so that the robot can easily detect its position in the camera image. Color range is tuned by trial and error so that it cannot be influenced by illumination changes caused by arm movements. There are tactile sensor units on its face. A total of 108 ($6 \times 6 \times 3$) green points in Figure 5(a) are given by the designer as reaching targets during random hand movements and placed at 0.02[m] intervals in the x, y, and z directions. The blue ball in Figure 5 (a) and (b) represent the gaze point of the two eyes.

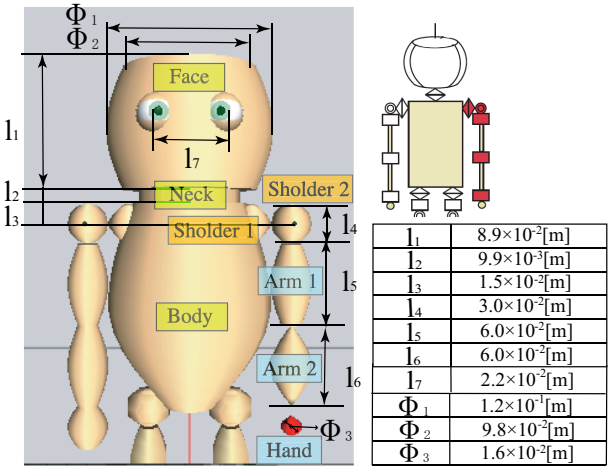

l_1	8.9×10^{-2}[m]
l_2	9.9×10^{-3}[m]
l_3	1.5×10^{-2}[m]
l_4	3.0×10^{-2}[m]
l_5	6.0×10^{-2}[m]
l_6	6.0×10^{-2}[m]
l_7	2.2×10^{-2}[m]
Φ_1	1.2×10^{-1}[m]
Φ_2	9.8×10^{-2}[m]
Φ_3	1.6×10^{-2}[m]

Mass

Face	6.5×10^{-1} [kg]	Neck	2.6×10^{-2} [kg]
Body	1.0 [kg]	Sholder 1	1.3×10^{-2} [kg]
Sholder 2	1.3×10^{-2} [kg]	Arm 1	2.6×10^{-2} [kg]
Arm 2	2.6×10^{-2} [kg]	Hand	1.3×10^{-2} [kg]

Fig. 4. Robot model and its specifications used in the experiments

B. Head-centered reference frame module

1) Arm posture space: Five joint angles of the left arm which are colored red in Figure 4 constitute the arm posture space. First, the robot selects one of the green points in front of the face randomly. The position of the selected point in the global reference frame (3-D Cartesian reference frame) is denoted as $\mathbf{X_{green}}$ and the hand position in the global reference frame is denoted as $\mathbf{X_{hand}}$. The following force $\mathbf{F_{hand}}$ is applied to the center of the hand. Since the initial position of the hand is near the waist, as shown in Figure 4, and all joints between hand and shoulder are free (no force is applied), an arm posture for each reaching target is uniquely determined.

$$\mathbf{F_{hand}} = a_1(\mathbf{X_{green}} - \mathbf{X_{hand}}) \tag{1}$$

where, a_1 is a positive constant and set to 75[N/m] here. When the hand reaches X_{green}, the robot selects other point again.

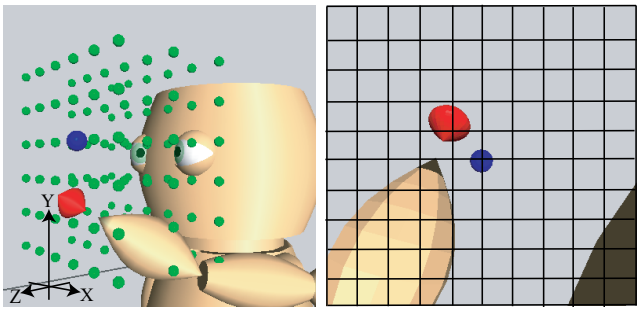

(a) The robot (b) Image space

Fig. 5. A simulation model:108 green points in (a) are given by the designer as reaching targets during random hand movements and placed at 0.02[m] intervals in the x, y, and z directions. The blue ball represents the gaze point of the two eyes. (b) Image space is the actual camera image divided into 10×10 units. The winner unit is the one in which the center of the hand is included.

Here, we focus on a self-organizing map (SOM) [18] algorithm to compress the data. The joint angle data are recorded and used as training data to construct the SOM as an arm posture space.

There is a representive vector for each unit of the arm posture space. The representive vector Θ_i for the i-th unit is

$$\mathbf{\Theta_i} = (\theta_1^i, \theta_2^i, ..., \theta_n^i). \tag{2}$$

where n is the number of joint angles (here, $n = 5$). When the current arm posture Θ is given,

$$\mathbf{\Theta} = (\theta_1, \theta_2, ..., \theta_n), \tag{3}$$

the mapping for the i-th unit on the space is updated depending on the distance from the winner c_{arm}-th unit,

$$\Delta\mathbf{\Theta}_i = \kappa(t)\exp(-\|i - c_{arm}\|/\gamma)(\mathbf{\Theta} - \mathbf{\Theta_i}), \tag{4}$$

$$c_{arm} = \arg\min_i \|\mathbf{\Theta} - \mathbf{\Theta}_i\|. \tag{5}$$

$\kappa(t)$ and γ are a learning rate that decays as the learning proceeds and a scaling factor, respectively. For example, in this case, $\kappa(t)$ is computed as following,

$$\kappa(t) = 0.4 \times exp(1.0 - t/500), \tag{6}$$

and the γ is set to 0.01. The size of the SOM is 10×10 and the learned map is shown in Figure 6 (a). The number of learning steps is 500. The map holds the similar representative vectors in neighboring units.

After learning, in each step, the Euclidean distance between the representative vector of the i-th unit and the actual arm posture is calculated. Then, using the winner unit (here the

c_{arm}-th unit) with the smallest Euclidean distance, activity α_i^{arm} of the i-th unit is given by

$$\alpha_i^{arm} = e^{-\beta(d_i^{arm})^2}, \tag{7}$$

$$d_i^{arm} = \|\mathbf{\Theta}_i - \mathbf{\Theta}_{c_{arm}}\|. \tag{8}$$

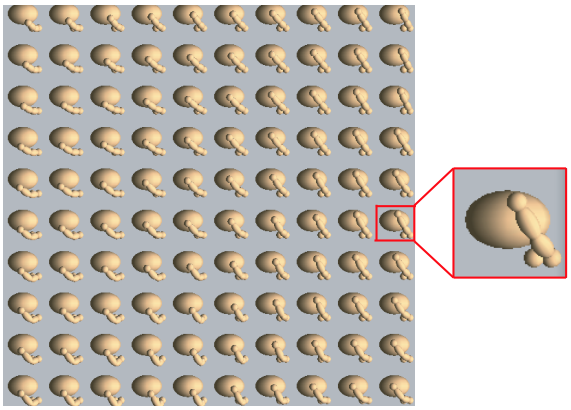

(a) Arm posture space

(b) Ocular angle space

Fig. 6. Acquired maps of arm posture space and ocular angle space

2) Ocular angle space: To collect the sets of the ocular angles and the location of the visual stimuli in the camera image, the robot records the ocular angles (pan-tilt angles of each eye) while simultaneously recording the arm joint angles. First, the position $\mathbf{X_{fixate}}$ in the global reference frame is defined as

$$\mathbf{X_{fixate}} = \mathbf{X_{hand}} + a_2\mathbf{R}, \tag{9}$$

$$\mathbf{X_{fixate}} = (X_{fixate}x, X_{fixate}y, X_{fixate}z), \tag{10}$$

$$\mathbf{R} = (Rx, Ry, Rz). \tag{11}$$

Rx and Ry are selected among the values from -1 to 1 randomly. Rz equals to 0 and a_2 is 0.05. We adopt this random noise $\mathbf{R}$ in order to duplicate a behavior of infants who cannot move eyeballs toward an object correctly. We denote the vector of the actual ocular angles $\mathbf{\Phi}$ and the position of eyes on the face $(\mathbf{X_{Reye}}, \mathbf{X_{Leye}})$ are given by:

$$\mathbf{\Phi} = (\phi_{right-pan}, \phi_{right-tilt}, \phi_{left-pan}, \phi_{left-tilt}), \tag{12}$$

$$\mathbf{X_{Reye}} = (X_{Reye}x, X_{Reye}y, X_{Reye}z), and \tag{13}$$

$$\mathbf{X_{Leye}} = (X_{Leye}x, X_{Leye}y, X_{Leye}z). \tag{14}$$

Then, ocular angles are given by:

$$\phi_{right-pan} = arctan(\frac{X_{fixate}x - X_{Reye}x}{X_{fixate}z - X_{Reye}z}), \tag{15}$$

$$\phi_{right-tilt} = arcsin(\frac{X_{fixate}y - X_{Reye}y}{\|\mathbf{X_{fixate}} - \mathbf{X_{Reye}}\|}), \tag{16}$$

$$\phi_{left-pan} = arctan(\frac{X_{fixate}x - X_{Leye}x}{X_{fixate}z - X_{Leye}z}), and \tag{17}$$

$$\phi_{left-tilt} = arcsin(\frac{X_{fixate}y - X_{Leye}y}{\|\mathbf{X_{fixate}} - \mathbf{X_{Leye}}\|}). \tag{18}$$

On the other hand, the robot cannot move its eyeballs to an object voluntarily based on the positions in the camera reference frame, which is the same situation as infants.

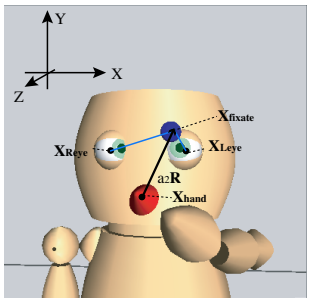

Fig. 7. Variables for the calculation of ocular angles

Recorded ocular data are used as training data to construct a SOM and the size is 15×15 as shown in Figure 6 (b). The number of learning steps is 1,000. After training, the winner unit, whose ID is c_{eye}, is computed in the same manner as for the arm posture space:

$$c_{eye} = \arg\min_i \|\mathbf{\Phi} - \mathbf{\Phi}_i\|, \tag{19}$$

where the representative vector is given by:

$$\mathbf{\Phi_i} = (\phi^i_{right-pan}, \phi^i_{right-tilt}, \phi^i_{left-pan}, \phi^i_{left-tilt}). \tag{20}$$

3) Image space: While recording the ocular data, the robot simultaneously detects its hand position in the camera reference frame. The right(left)-eye image space is the actual camera image divided into 10×10 units as shown in Figure 5(b). The winner unit whose ID is $c_{rightimage}(c_{leftimage})$ is the one in which the center of the hand area is included. We adopt the demarcated parts instead of coordinates in the camera image in order to decrease the amount of information to deal with.

4) Eye information space: In the next step, the eye information space is prepared to combine the activating patterns in the three spaces of the ocular angle space, the right-eye space, and the left-eye image space. A SOM [18] is constructed by utilizing the IDs of the winner units in these three spaces, $C = (c_{eye}, c_{rightimage}, c_{leftimage})$, as the representative vector in the same way shown in subsection *B.1)*. The size is 20×20 and the number of learning steps is 1,000. The winner unit whose ID of this space is denoted as $c_{eyeinfo}$ and the activity $\alpha_i^{eyeinfo}$ of the eye information space are defined in the same manner as Eqs. (7) and (8).

5) Head-centered visual space: Finally, in the head-centered visual space, the robot learns the association of these combinations of ocular angles and image information to code the same location in the head-centered reference frame by using the proprioception (arm joint angles) as a reference information. The units of the head-centered visual space connect to the units of the arm posture space in a one-to-one correspondence. Then, activity α_i^{space} of the head-centered visual space is

$$\alpha_i^{space} = \alpha_i^{arm}. \tag{21}$$

The robot hand is moved toward the green points and its gaze point around the hand in the same way as learning the ocular angle space and arm posture space in subsections *B.1)* and *2)*. Meanwhile the robot learns the association between head-centered space and the eye information space based on Hebbian learning [25] which is modeled after the synaptic connections in the brain. It is basically an unsupervised training algorithm in which the strength of a connection (weight between units) is increased if both neurons (units) are active at the same time. The original hebbian rule itself has no mechanism for connection weights to get weaker and no upper bound for how strong they can get and is therefore unstable. Therefore some modified approaches were suggested. In this model, we use Von Der Malsburg's method [26] that maintains a constant integration of all connection strengths to the same neuron through normalization.

All units of two spaces are connected to each other and the connection weight between the i-th unit in the eye information space and the j-th unit in the head-centered visual space, w_{ij}^{space}, is updated based on Eqs. (22)-(24):

$$\bar{w_{ij}^{space}}(t+1) = \frac{w_{ij}^{space}(t+1)}{\sum_{j=0}^{N_1} w_{ij}^{space}(t+1)}, \tag{22}$$

where

$$w_{ij}^{space}(t+1) = w_{ij}^{space}(t) + \Delta w_{ij}^{space}, and \tag{23}$$

$$\Delta w_{ij}^{space} = \epsilon_1 \alpha_i^{space} \alpha_j^{eyeinfo}. \tag{24}$$

N_1 and ϵ_1 are the number of units of the head-centered visual space (here, 100) and a learning rate (here, 0.2), respectively. After learning this association, the robot records the $c_{act-space}$-th unit that is most strongly connected to the $c_{eyeinfo}$-th unit.

C. VIP module

In the VIP module, the robot integrates the tactile stimuli of the face and the visual stimuli that are specified in the head-centered reference frame through tactile experience.

1) Visual trajectory space: This space is prepared for classifying the historical data of approaching visual stimuli whose positions can be computed in the head-centered reference module. First, the robot repeatedly moves its hand toward a random position on the surface of its face from the front. In this case, the gaze point is moved in the same way as before. At that time, the robot computes $c_{act-space}$ that has the strongest connection to $c_{eyeinfo}$ by using the input data of the ocular angles and the positions in the camera reference frame in every step. Then, the trajectory of the last three steps $(c_{act-space}(t-2), c_{act-space}(t-1), c_{act-space}(t))$ is achieved and used as the representative vector to construct another SOM (visual trajectory space). t is the time when the hand gets within 0.02[m] of the face. The size of the map is 10×10.

After acquiring SOM, activity α_i^{traj} of the visual trajectory space is calculated when the hand touches the face.

2) Tactile space: The sensor units on the surface of the face correspond to units in tactile space. If the robot perceives tactile stimuli within period t_{const} after t, the ID of the actual activated c_{tac}-th unit in the tactile space is recorded as a winner unit. Additionally, the activity of the i-th unit of tactile space is calculated based on c_{tac}:

$$\alpha_i^{tac} = e^{-\zeta (d_i^{tac})^2}, \tag{25}$$

$$d_i^{tac} = \|i - c_{tac}\|. \tag{26}$$

3) Integration (VIP) space: In this case, the tactile space units are connected to those in the integration (VIP) space as a one-to-one correspondence. Activity α_i^{vip} in the latter space is given by:

$$\alpha_i^{vip} = \alpha_i^{tac}. \tag{27}$$

The robot learns the association between the visual trajectory space and the integration (VIP) space based on Hebbian learning. The connection weight between the i-th unit in the visual trajectory space and the j-th unit in the integration (VIP) space, w_{ij}^{vip}, is updated based on Eqs. (28)-(30):

$$\bar{w_{ij}}^{vip}(t+1) = \frac{w_{ij}^{vip}(t+1)}{\sum_{i=0}^{N_2} w_{ij}^{vip}(t+1)}, \tag{28}$$

where

$$w_{ij}^{vip}(t+1) = w_{ij}^{vip}(t) + \Delta w_{ij}^{vip}, and \tag{29}$$

$$\Delta w_{ij}^{vip} = \epsilon_2 \alpha_i^{traj} \alpha_j^{vip}. \tag{30}$$

N_2 is the number of units of visual trajectory space and set to 100. ϵ_2 is the learning rate and set to 0.5.

Finally, by calculating the $c_{act-vip}$-th unit that is most strongly connected to c_{traj}-th unit, the robot can estimate the tactile sensor units that are going to be hit by the hand.

IV. EXPERIMENTAL RESULTS

A. Head-centered reference frame module

The proposed neural learning architecture described above is applied to the simulation model. First, to evaluate the learning maturation of Hebbian learning in the head-centered visual space, the averaged variance of weights w_{ij}^{space} of the connection between one unit of the eye information space and all units of the head-centered visual space is calculated. In this case, the robot learns the association between two spaces when the hand touches a green point. Initially, one unit of the former space is associated with all units of the latter space equally: therefore the variance is still large. However during learning, the stronger the connection becomes between one unit of the former space and the appropriate unit of the latter space, the smaller the averaged variance becomes.

The averaged position on the head-centered visual space, $\bar{\boldsymbol{r}}^i$, which is connected from the i-th unit of the eye information space is calculated as

$$\bar{\boldsymbol{r}}^i = \frac{\sum_{j=1}^{N_1} w_{ij}^{space} \boldsymbol{r}_j}{\sum_{j=1}^{N_1} w_{ij}^{space}}, \tag{31}$$

where $\boldsymbol{r}_j$ denotes the position vector of the j-th unit on the head-centered visual space. Furthermore, the variance of connection weights, $\hat{r}^i$, is calculated as

$$(\hat{r}^i)^2 = \frac{\sum_{j=1}^{N_1} w_{ij}^{space} \|\boldsymbol{r}_j - \bar{\boldsymbol{r}}^i\|^2}{\sum_{j=1}^{N_1} w_{ij}^{space}}. \tag{32}$$

Then, the connection-weight evaluation is performed with

$$R_1 = \frac{\sum_{i=1}^{N_3} \hat{r}^i}{N_3}, \tag{33}$$

where N_3 is the number of units of eye information space and set to 400. The result of 6000 steps during learning is shown in Figure 8. As learning proceeds, the variance converges and the connections between the units seem potentiated.

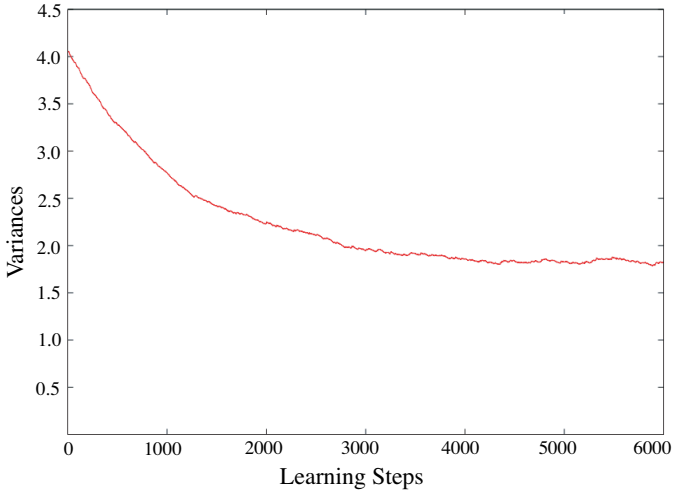

Fig. 8. Variances of the weights during the Hebbian learning of the association between the eye information and the head-centered visual spaces.

We also investigated how the robot adapts itself to situations in which its hand position in the head-centered reference frame is the same although the sets of ocular angles and positions in the camera image are different as shown in Figure 2. As indicated in Figure 9 (a), the robot places its hand at the fixed point and moves its gazing point for 300 steps as plotted with blue lines. Concretely speaking, in each step, the robot calculates $c_{eyeinfo}$ using the perceived sensation of $c_{eye}, c_{rightimage}, c_{leftimage}$ that are obtained from the actual gaze angles and camera images. Then, in the head-centered visual space, $c_{act-space}$ is determined. Moreover, by assigning the representative vector $\boldsymbol{\Theta}_{\boldsymbol{c_{act-arm}}} = (\theta_1^{c_{act-arm}}, ..., \theta_n^{c_{act-arm}})$ of the $c_{act-arm}$-th unit in the arm posture space that is interlinked to $c_{act-space}$ to Eq. (34), the position of the hand $\boldsymbol{X}_{\boldsymbol{c_{act-arm}}} = (x_{c_{act-arm}}, y_{c_{act-arm}}, z_{c_{act-arm}})$ in the global reference frame (3-D Cartesian reference frame) is calculated as following,

$$\boldsymbol{X}_{\boldsymbol{c_{act-arm}}} = f(\boldsymbol{\Theta}_{\boldsymbol{c_{act-arm}}}). \tag{34}$$

where f is a function that transforms joint angles and link lengths into the hand position in the global reference frame. It is given just to examine the learning results by the designer. In this case, the x, y, and z directions are shown in Figure 5(a). In order to investigate how the learning proceeds over the time, the robot records the connection weight values at learning steps = 1000, 2000, 3000, and 6000. Then, after learning, we make the robot compute $c_{act-space}$ and the hand positions $X_{c_{act-arm}}$ subsequently based on these four recorded connection weight values. In each step, the moving average of $\boldsymbol{X}_{\boldsymbol{c_{act-arm}}}$ in the last four steps is computed and indicated as the light blue point in Figures 9(b)-(e) and in Figure 10. The robot can approximately recall the arm posture that resembles the actual one from the ocular angles and the positions in the camera image that are different from one observation to another. As the learning proceeds, these estimated positions seem to slowly converge to the hand position.

In addition, the histogram of differences (errors) between $\boldsymbol{X}_{\boldsymbol{c_{act-arm}}}$ and the positions of the actual hand in Figure 9(e) is shown in Figure 10. The average values of 300 errors for the three directions are $0.01034[m]$(x axis), $0.01057[m]$(y), and $0.01289[m]$(z), and the mean error of the z direction is bigger than the others. One reason could be that the number of units in the eye information space is insufficient to cover a large amount of training data.

Finally, $\boldsymbol{X}_{\boldsymbol{c_{act-arm}}}$ and the actual hand positions while the hand is moved toward the green points in order are shown in Figure 11, where the errors in z direction are bigger than the others also in this case.

B. VIP module

To check the Hebbian learning maturation in the integration (VIP) space, the averaged variance of the weights of the connection between the one unit of the integration (VIP) space and all units of the visual trajectory is computed in the same manner as shown in the last section. The variances of 2,000 steps during learning are shown in Figure 12. As learning proceeds, the connection between the units is evaluated to be potentiated.

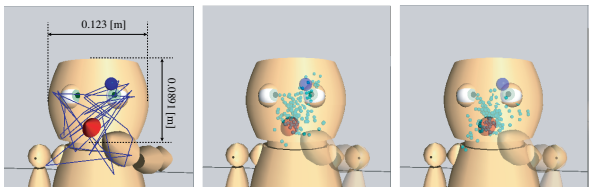

(a) Trajectory of gazing points

(b) The estimated position (1000th step)

(c) The estimated position (2000th step)

(d) The estimated position (3000th step)

(e) The estimated position (6000th steps)

Fig. 9. Estimated hand positions while robot randomly moves its gaze point around the hand by using the weight values acquired in 1000th, 2000th, 3000th, and 6000th step. : blue lines show trajectory of 200 gaze points (blue ball) and light blue points show estimated hand positions.

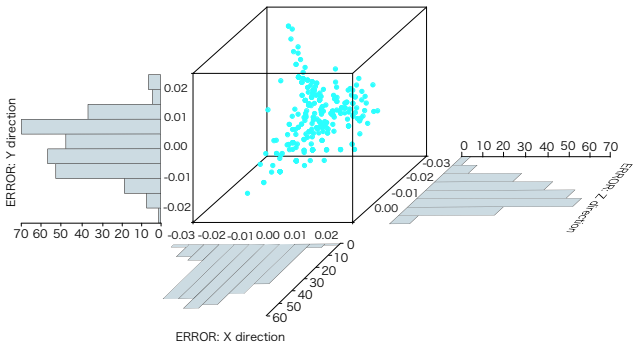

Fig. 10. Histogram of differences between actual and estimated hand positions for Figure 8 (e)

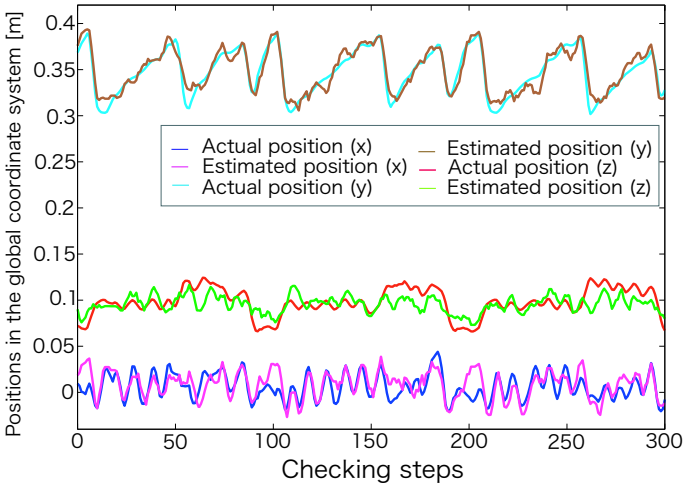

Fig. 11. Difference between the actual and estimated hand positions (while the robot is moving its hand)

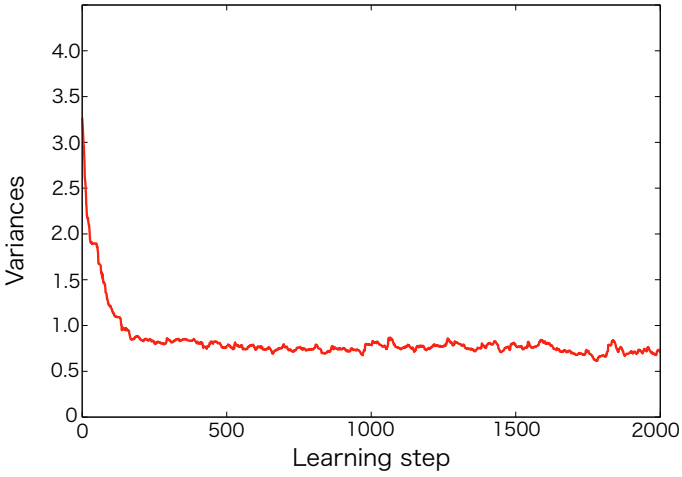

Fig. 12. Variances of the weights during the Hebbian learning of the association between the VIP and the visual trajectory spaces

Next, we investigated whether the integration space of the VIP module has the same function as VIP neurons themselves and whether the robot can estimate the tactile units that are going to be activated regardless of the positions of the gaze point. In Figure 13(a), we placed the screen in front of the robot as seen in the observation of monkeys in Figure 2 and its center is the midpoint of the two eyes. The tactile sensor units are located as indicated in Figure 13(b) on the surface of the face. During the hand movement to the face as explained before, we visualize the level of each weight using the green color connected to the c_{traj}-th unit in the visual trajectory space as shown in Figure 13(a), 14(III). They are compared with visual and somatosensory receptive fields of VIP neurons. The red arrow indicates the trajectory of the hand. In Figure 14

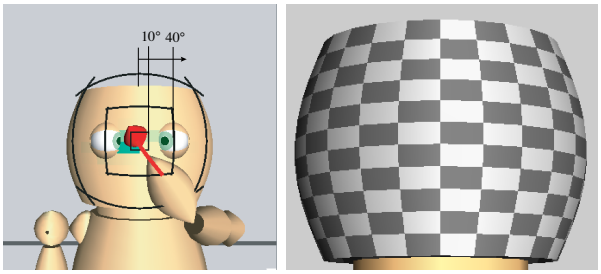

(a) Screen in front of the face

(b) Tactile sensor units

Fig. 13. (a) The robot moves its hand toward the face randomly and estimates the position that is going to be activated by the contact by calculating the unit that has a big weight value between the winner c_{traj}-th unit in the visual trajectory space. The screen is placed in front of the face and the results are compared with the finding of VIP neurons. (b) Tactile sensor units on the face.

(I) and (II), some examples of two kinds of receptive fields that VIP neurons have are shown. Moreover, Figures 14 (III) are the activated tactile units at the time when the visual stimuli (the own hand in this case) are shown in each visual receptive field in (I). In Figure 14 (III-f), when the hand is moved toward

the bottom of the right eye, an error is observed. However, the robot can roughly estimate the tactile units that are going to be activated regardless of the position of the gaze point as a result. It seems that the area including the units that connects strongly with the c_{traj}-th unit resembles the corresponding tactile receptive field of the neuron. It could be mentioned that the function of our VIP module is qualitatively similar to actual VIP neurons.

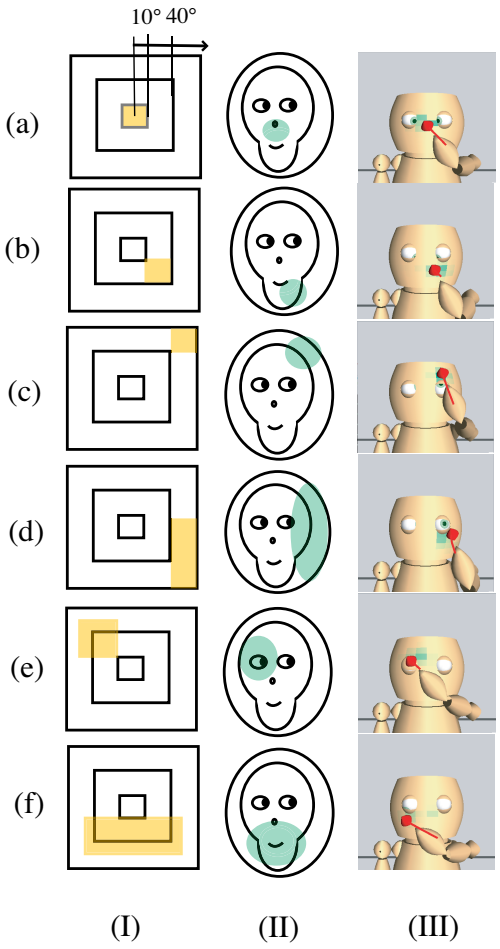

Fig. 14. (I)This square can be thought of as a screen placed in front of the face as seen in Figure 12. On the square, the patch of orange color corresponds to the visual receptive fields of VIP neurons. (II)The patch of blue color corresponds to the somatosensory receptive field of the same neuron. (III)The activated tactile units at that time when the visual stimuli (the own hand in this case) are indicated in each visual receptive field in (I).

Furthermore, we investigate how the errors in estimating the activating units are being reduced over learning time. The several weight values, $w_{ij}^{vip}(t = 100, 300, 500, 1000, and 2000)$ are recorded in learning phase and used to compute $c_{act-vip}$ while the robot is moving its hand toward the face randomly for 200 steps. Figure 15 shows the histogram of the Euclidean distances of the IDs ($c_{act-vip}$ and c_{tac}) based on each weight value. It appears the accuracy of estimation is enhanced gradually as learning proceeds. Figure 16 (a) shows the final result when utilizing the weight $w_{ij}^{vip}(2000)$. There are a few errors and they probably happened because the training data of the visual trajectory space, $c_{act-space}(t-2), c_{act-space}(t-1)$, and $c_{act-space}(t)$, were influenced by the errors of the head-centered visual space. Another reason is suggested that the robot sometimes loses sight of its hand by moving it outside of the field of view while recording the trajectory. Then, we did an experiment using only the proprioceptive input for VIP module. For the robot, it might be able to ascertain whether it is also possible to predict where the hand will hit without visual information. As stated in the section III. *B. 5)*, the units of the head-centered visual space connect to the units of the arm posture space in an one-to-one correspondence as,

$$c_{act-space}(t) = c_{arm}(t). \tag{35}$$

Therefore the visual trajectory space is retrained by calculating the historical pattern of the winner c_{arm} units here. In this way, the association between the visual trajectory space and the integration (VIP) space and the active tactile units are also estimated based on the activity determined by actual joint angles originally. In this case, the histogram of distances of IDs of the activated and estimated tactile units is shown in Figure 16 (b). The accuracy of prediction is improved.

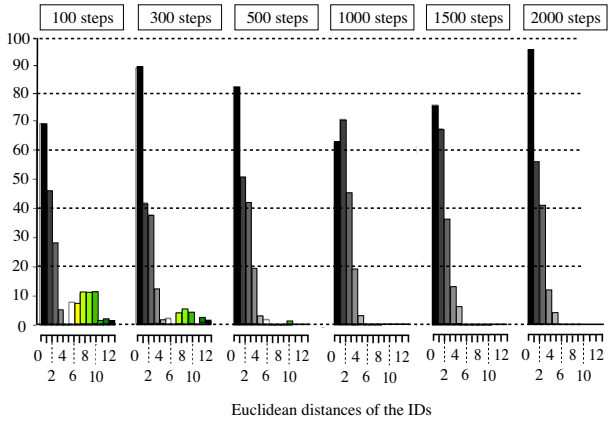

Fig. 15. The activated tactile units are estimated based on the weight values $w_{ij}^{vip}(100), w_{ij}^{vip}(300), w_{ij}^{vip}(500), w_{ij}^{vip}(1000), w_{ij}^{vip}(1500), w_{ij}^{vip}(2000)$. These are histograms of differences between the actual activated and estimated units of tactile space.

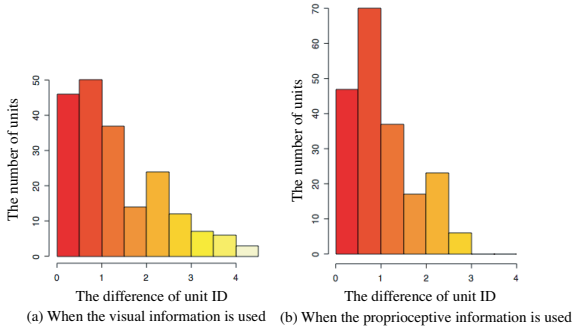

Fig. 16. Histogram of differences between the actual activated and estimated units of tactile space

V. Conclusion and Discussion

In this paper, we proposed a learning model in which the visuo-spatial and body representations are acquired through

"hand regard" behavior that can be observed in the human developmental process. Consequently, the robot acquired a form of perception in which the surrounding space is roughly encoded in a head-centered reference frame. It can also integrate the visual stimuli coded in this reference frame with tactile stimuli on the face, and can acquire the representation whose function is similar to that of VIP neurons by using SOM and Hebbian learning hierarchically.

As a model of acquisition of facial multi-modal representation in cognitive developmental robotics, there is a method that Fuke et al. [16] proposed so far. In that study, the robot can learn the relative arrangement of tactile sensors on the face. However, because the relationship between these tactile sensors and stimuli in the surrounding space is not considered, it is difficult to utilize the representation for motion generation such as guiding head movements. On the other hand, the representation in this study can be useful to estimate an approaching object. In the future, avoidance behavior might be able to be constructed based on it. In addition, by implementing this method in existing studies, robots can acquire more practical body representations. For example, Hikita et al [27] proposed a method which enables a robot to associate a position of an end effector (hand or tip of tools) in the camera image with the proprioception of its arm. If this "position" can be represented in the head-centered reference frame (or body-centered reference frame in the future) based on our method, it is expected that the robot becomes able to detect the end effectors in a wider area by using the eyeball and neck angles effectively.

There are three issues that we should tackle in the future. First, there are still some errors that can be seen in Figures 9 and 16. We are going to try to use other algorithm to improve it. There is a possibility that normalizing rules of Hebbian learning negatively affect the maturation. Therefore, for example, we will try to apply the trace rule [28] that is a modified Hebbian rule and changes synaptic weights according to both the current firing rate and the firing rates to recently observed stimuli. This enables neurons to learn to respond similarly to the gradually transforming inputs it receives.

Secondly, we construct SOMs hierarchically and their sizes are determined by trial and error. If the size is small, the representive vectors become too generalized. Especially in the case of the eye information space, it is not always true that the hand positions in the space are next to each other when the relative vectors of the units of the eye information space are similar. If the size is too big, it is difficult for one unit to encode the visuo-spatial representation as a cluster like visual and tactile receptive fields of neurons. However, it can be resolved by adjusting the parameter of the activity of units in the spaces such as β. Then, sizes of SOMs have to be examined carefully because there is a possibility that it causes some errors. So far, we have not implemented an algorithm to explore the most appropriate size to cluster the data satisfactorily. However, when we try to scale up this model to larger tactile spaces and other representations in other kinds of reference frames in the future, it might still be an issue how the sizes are optimized and vast amounts of data should be compressed. We are working on a method in which the robot can determine the size that is adequate enough to cover all input data autonomously and, at the same time, consider other algorithms for compression such as deep belief nets [29].

Finally, in the present study, a robot hand is moved in the small space in front of the face by giving a force only to the hand. Then, the arm postures that provide a hand position is specified. On the other hand, if joint angles are randomly selected, it is difficult to utilize them in order to represent the same position. In case of human infants, before the hand regard behavior starts to be observed, they tend to acquire some kinds of motor primitives based on the physical interaction between body and environment, and the effect of gravity. Thus, it is highly probable that the actual infant hand position correlates with the arm posture during hand regard behavior too. We are going to discuss a relationship between the acquisition of motor representation and visuo-spatial representation in the next stage.

Next, not only to improve the model but also to understand the human mechanism in more detail, it is also important to approach the problem of how a robot can find the object that it should pay attention to as reference information for the acquisition of the head-centered or other reference frames. For example, in our study, the proprioception of the arm was set to be adopted as reference information by the designer. But, if the robot is able to select an object in the surrounding space as reference information autonomously based on an internal attention mechanism, we can also discuss the acquisition of visuo-spatial representation of extra-personal space. It might be required that the robot can predict the change of the visual information (optical flow) in the image from the ocular motor information and have the memory system at that time.

As the main topic in this paper was first inspired by some findings of humans, finally we try to compare functions of each space in this model to those of some regions that are found in the neurophysiological studies here. First, we pay attention to some findings about LIP (lateral intraparietal) area [30]. Andersen [31] found neurons in the monkey parietal cortex area, LIP area, that combine three kinds of signals: the position of the stimulus on the retina, the positions of the eyes in the orbit and the neck angles. The LIP area connects to the VIP area [32] and is reported to have both eye-centered and head-centered visual receptive fields [33]. The head movement is not dealt with in our study, but, it can be assumed that the eye information space corresponds to the LIP area as shown in Figure 14. As mentioned in the introduction, VIP area is known as the region that has the "peri-personal" visuo-spatial representation. The "peri-personal space" is defined as the space within reach of the arm in the neurophysiological studies. Actually, it was revealed that the visuospace is represented in different regions in the brain, peri-personal space [23] and extra-personal space that is out of reach of the arm [34] based on the findings of spatial neglect syndromes. This peri-personal space is extended when the subject uses a tool [35]. Rizolaatti et al. [36] also reported that connection of this VIP area and the F4 area (the area of arm representation) in the brain is important for that representation. Thus, we also suppose that arm posture space corresponds to the F4 area (the area of arm representation) and their claim

might support our hypothesis in which the arm proprioceptive information contribute to the construction of visuo-spatial representation.

REFERENCES

[1] H. Head and G. Holmes. Sensory disturbances from cerebral lesions. *Brain*, 34:102–254, 1911/1912.

[2] S. I. Maxim. *Body Image and Body Schema (edited by P. D. Helena)*. John Benjamins Publishing Company, 2005.

[3] V. S. Ramachandran and S. Blakeslee. *Phantoms in the Brain: Probing the Mysteries of the Human mind*, volume 2. William Mollow, New York, 1998.

[4] A. Iriki, M. Tanaka, S. Obayashi, and Y. Iwamura. Self-images in the video monitor coded by monkey intraparietal neurons. *Neuroscience Research*, 40:163–173, 2001.

[5] T. Jellema, G. Maassen, and D. I. Perrett. Single cell integration and aminate form, motion and location in the superior temporal cortex of the macaque monkey. *Cerebral Cortex*, 14:781–790, 2004.

[6] J. R. Duhamel, C. L. Colby, and M. E. Goldberg. Ventral intraparietal area of the macaque: Congruent visual and somatic response properties. *Journal of Neurophysiology*, 79:126–136, 1998.

[7] M. S. A. Graziano and D. F. Cooke. Parieto-frontal interactions, personal space, and defensive behavior. *Journal of Neuropsychologia*, 44:845–859, 2006.

[8] M. I. sereno and R. Huang. A human parietal face area contains aligne d head-centered visual and tactile maps. *Nature Neuroscience*, 9:1337–1343, 2006.

[9] G. M. Stratton. Vision without inversion of the retinal image. *Psychological review*, 4:463–481, 1897.

[10] M. Asada, K. F. MacDorman, H. Ishiguro, and Y. Kuniyoshi. Cognitive developmental robotics as a new paradigm for the design of humanoid robots. *Robotics and Autonomous System*, 37:185–193, 2001.

[11] Y. Yoshikawa. Subjective robot imitation by finding invariance. *Ph. D thesis, Osaka University*, 2005.

[12] C. Nabeshima, M. Lungarella, and Y. Kuniyoshi. Body schema adaptation for robotic tool use. *Advanced Robotics*, 20:1105–1126, 2006.

[13] A. Stoytchev. Toward video-guided robot behaviors. *Proceedings of the 7th International Conference on Epigenetic Robotics*, pages 165–172, 2007.

[14] L. Natale, F. Orabona, G. Metta, and G. Sandini. Sensorimotor coordination in a "baby" robot: learning about objects through grasping. *Robotics and Autonomous System*, 37:185–193, 2001.

[15] M. Hersch, E. Sauser, and A. Billard. Online learning of the body schema. *International Journal of Humanoid Robotics*, 5(2), 2008.

[16] S. Fuke, M. Ogino, and M. Asada. Body image constructed from motor and tactile images with visual information. *International Journal of Humanoid Robotics (IJHR)*, 4(3):347–364, 2007.

[17] A. Pouget, S. Deneve, and J. R. Duhamel. A computational perspective on the neural basis of multisensory spatial representations. *Nature Reviews Neuroscience*, 3:741–747, 2002.

[18] T. Kohonen. Self-organizing maps. *Springer-Verlag Verlin Heidelverg*, 1995.

[19] T. N. Aflalo and M. S. A. Graziano. Possible origins of the complex topographic organization of motor cortex: Reduction of a multidimensional space onto a two-dimensional array. *The Journal of Neuroscience*, 26(23):6288–6297, 2006.

[20] R. O. Gilmore and M. H. Johnson. Body-centered representations for visually-guided action emerge during early infancy. *Cognition*, 65,1:1–9, 1997.

[21] J. Piaget. *La Naissance de l'intelligence chez l'enfant*. Delachaux et Niestle, 1936.

[22] G. Rizzolatti, C. Sinigaglia, and F. Anderson. *Mirrors in the brain - How our Minds Share Actions and Emotions*. Oxford University Press, Great Britain, 2007.

[23] P. W. Halligan and J. C. Marshall. Left neglect for near but not for far space in man. *Nature*, 352:673–674, 1991.

[24] R. Featherstone. The calculation of robot dynamics using articulated-body inertias. *The International Journal of Robotics Research*, 2(1):13–30, 1983.

[25] D. O. Hebb. *The organization of behavior*. Wiley, New York, 1949.

[26] Von Der Malsburg. Self-organization of orientation sensitive cells in the striate cortex. *Kybemetic*, 14:85–100, 1973.

[27] M. Hikita, S. Fuke, M. Ogino, T. Minato, and M. Asada. Visual attention by saliency leads cross-modal body representaion. *Proceedings of the 7th International Conference on Development and Learning*, pages 157–162, 2008.

[28] P. Foldiak. Learning invariance from transformation sequences. *Neural Computation*, 3(2):194–200, 1991.

[29] G. E. Hinton, S. Osindero, and Y. Teh. A fast learning algorithm for deep belief nets. *Neural computation*, 18(7):1527–1554, 2006.

[30] D. J. Freedman and J. A. Assad. Experience-dependent representation of visual categories in parietal cortex. *Nature*, 443:85–88, 1988.

[31] R. A. Andersen. Encoding of intention and spatial location in the posterior parietal cortex. *Cerebral Cortex*, 5:457–469, 1995.

[32] G. J. Bratt, R. A. Andersen, and J. R. Stoner. Visual receptive field organization and cortico-cortical connections of the lateral intraparietal are (area lip) in the macaque. *The journal of comparative neurology*, 299:421–445, 1990.

[33] O. A. Mullette-Gillman, Y. E. Cohen, and J. M. Groh. Eye-centered, head-centered, and complex coding of visual and auditory targets in the intraparietal sulcus. *Journal of Neurophysiology*, 94:2331–2352, 2005.

[34] A. Cowey, M. Small, and S. Ellis. Left visuo-spatial neglect can be worse in far than in near space. *Neuropsychologia*, 32:1069–1066, 1994.

[35] A. Berti and F. Franssinetti. When far becomes near: Remapping of space by tool use. *Journal of Cognitive Neuroscience*, 12:415–420, 2000.

[36] G. Rizzolatti and M. Matelli. Two different streams form the dorsal visual system: anatomy and functions.

Experimental Brain Research, 153:146–157, 2003.